FULL PAPER

BJC

British Journal of Cancer (2016) 115, 354–363 | doi: 10.1038/bjc.2016.179

Keywords: microRNA; *miR-26a-5p*; *miR-26b-5p*; *PLOD2*; bladder cancer; tumour suppressor

Tumour-suppressive *miRNA-26a-5p* and *miR-26b-5p* inhibit cell aggressiveness by regulating *PLOD2* in bladder cancer

K Miyamoto[1], N Seki[2], R Matsushita[1], M Yonemori[1], H Yoshino[1], M Nakagawa[1] and H Enokida*[,1]

[1]*Department of Urology, Graduate School of Medical and Dental Sciences, Kagoshima University, 8-35-1 Sakuragaoka, Kagoshima 890-8520, Japan and* [2]*Department of Functional Genomics, Chiba University Graduate School of Medicine, 1-8-1 Inohana, Chuo-ku, Chiba 260-8670, Japan*

Background: Previous studies have revealed that *miR-26a-5p* and *miR-26b-5p* act as tumour suppressors in various types of cancer tissues. Here, we aimed to investigate the functional roles of these miRNAs and to identify their regulatory targets in bladder cancer (BC).

Methods: We performed functional assays in BC cells using transfection of mature microRNAs (miRNAs). *In silico* and luciferase reporter analyses were applied to identify target genes of these miRNAs. The overall survival (OS) of patients with BC was evaluated by the Kaplan–Meier method.

Results: *miR-26a-5p* and *miR-26b-5p* were significantly downregulated in BC tissues. Restoration of these miRNAs inhibited cell migration and invasion in BC. The gene encoding procollagen-lysine, 2-oxoglutarate 5-dioxygenase 2 (*PLOD2*), a collagen crosslinking enzyme, was directly regulated by *miR-26a-5p* and *miR-26b-5p*. Kaplan–Meier analysis revealed that patients with high *PLOD2* expression had significantly shorter OS compared with those with low *PLOD2* expression ($P = 0.0153$).

Conclusions: *PLOD2*, which is associated with the stiffness of the extracellular matrix, was directly regulated by *miR-26a-5p* and *miR-26b-5p* and may be a good prognostic marker in patients with BC.

In developed countries, bladder cancer (BC) is the fifth most commonly diagnosed cancer (Siegel *et al*, 2012). Bladder cancer can be categorised as non-muscle-invasive BC (NMIBC) and muscle-invasive BC (MIBC); the 5-year survival rates for patients with MIBC and NMIBC are 60% and 90%, respectively (Zuiverloon *et al*, 2012). Nearly 80% of patients with distant metastases die in the first 5 years after diagnosis (Meeks *et al*, 2012). The molecular mechanisms of recurrence and metastasis in BC are not well understood. Previous studies have not yet identified effective chemotherapies for advanced BC (Bellmunt and Petrylak, 2012). Thus, although patients with advanced BC are generally treated with chemotherapy using gemcitabine and cisplatin, progression-free survival is short (De Santis *et al*, 2012). Most clinical trials evaluating chemotherapies or molecular-targeted therapeutics for advanced BC have shown limited benefits, and there are currently no effective second-line chemotherapies available (Ghosh *et al*, 2014). Therefore, novel prognostic markers and effective treatment strategies based on RNA network studies are needed to improve outcomes in patients with BC.

MicroRNAs (miRNAs) are small noncoding RNAs (19–22 bases in length) that regulate protein-coding genes by binding to the 3′-untranslated region (UTR) of the target mRNA, thereby inhibiting transcription (Bartel, 2004; Carthew and Sontheimer, 2009). Previous studies have shown that miRNAs are aberrantly expressed in various human cancers and have significant roles in human oncogenesis and metastasis (Di Leva and Croce, 2010). Therefore, detection of aberrantly expressed miRNAs is an important first step in the elucidation of miRNA-regulated oncogenic pathways.

*Correspondence: Dr H Enokida; E-mail: enokida@m.kufm.kagoshima-u.ac.jp

Received 29 March 2016; revised 5 May 2016; accepted 17 May 2016; published online 16 June 2016

Our laboratory has characterised the miRNA expression signatures of several human cancers and revealed that *miR-26a-5p* and *miR-26b-5p* are frequently downregulated in various types of cancer, suggesting that these miRNAs function as tumour suppressors by targeting multiple oncogenes (Fukumoto *et al*, 2015; Kato *et al*, 2015). However, the functional roles of these miRNAs in BC are unclear. The aim of the present study was to investigate the functional roles of *miR-26a-5p* and *miR-26b-5p* and to identify their molecular targets in BC cells. Our data demonstrated that *miR-26a-5p* and *miR-26b-5p* were significantly downregulated in clinical BC specimens and that transfection of BC cells with these miRNAs significantly inhibited cancer cell migration and invasion. *In silico* analyses suggested that the gene encoding procollagen-lysine, 2-oxoglutarate 5-dioxygenase 2 (*PLOD2*), a collagen crosslinking enzyme, was a promising candidate target gene of these miRNAs. *PLOD2* has been shown to be associated with extracellular matrix (ECM) stiffness and dysregulation of the ECM (Gilkes *et al*, 2014). The discovery of molecular targets regulated by tumour-suppressive miRNAs provides important insights into the potential mechanisms of BC oncogenesis and suggests novel therapeutic strategies for the treatment of BC.

MATERIALS AND METHODS

Clinical specimens and cell culture. The tissue specimens for quantitative real-time reverse transcription–polymerase chain reaction (qRT–PCR) were collected from patients with BC ($n=69$) who had received cystectomy ($n=10$) or transurethral resection of their bladder tumours (TURBT; $n=59$) at the Kagoshima University Hospital between 2003 and 2015. Normal bladder epithelia ($n=23$) were derived from patients with noncancerous disease. The specimens were staged according to the American Joint Committee on Cancer-Union Internationale Contre le Cancer tumour-node-metastasis (TNM) classification and histologically graded (Sobin and Compton, 2010). Our study was approved by the Bioethics Committee of the Kagoshima University; written prior informed consent and approval were obtained from all patients. Patient details and clinicopathological characteristics are summarised in Supplementary Table 1. The median follow-up of the patients was 45.8 months.

The human BC cell lines T24 and BOY were maintained in the recommended medium containing 10% foetal bovine serum, 50 μg ml^{-1} streptomycin, and 50 U ml^{-1} penicillin in a humidified atmosphere of 95% air/5% CO_2 at 37 °C. Routine tests for mycoplasma infection were negative (Inoguchi *et al*, 2014; Itesako *et al*, 2014).

Tissue collection and RNA extraction. Tissues were immersed in RNAlater (Thermo Fisher Scientific, Waltham, MA, USA) and stored at −20 °C until RNA extraction. Total RNA, including miRNA, was extracted using a mirVana miRNA Isolation Kit (Thermo Fisher Scientific) following the manufacturer's protocol.

qRT–PCR. Stem-loop RT–PCR (TaqMan MicroRNA Assays; P/N: 000405 for *miR-26a-5p*, and P/N: 000407 for *miR-26b-5p*; Applied Biosystems, Foster City, CA, USA) was used to quantify miRNAs according to previously published conditions (Ichimi *et al*, 2009). TaqMan probes and primers for *PLOD2* (P/N: Hs 01118190_m1; Applied Biosystems) were assay-on-demand gene expression products. We used human *GUSB* (P/N: Hs99999908_m1; Applied Biosystems) and *RNU48* (P/N: 001006; Applied Biosystems) as internal controls, and the ΔCt method was used to calculate the fold changes relative to the expression levels of internal controls.

Transfection with mature miRNA and siRNA. As described elsewhere (Ichimi *et al*, 2009; Yoshino *et al*, 2011), T24 and BOY cells were transfected with Lipofectamine RNAiMAX transfection reagent (Thermo Fisher Scientific) and Opti-MEM (Thermo Fisher Scientific) with 10 nM mature miRNA. Mature miRNA and negative-control miRNA (Applied Biosystems) were used in gain-of-function experiments, whereas *PLOD2* small interfering RNA (siRNA) (cat. nos HSS108124 and HSS108125; Thermo Fisher Scientific) and negative-control siRNA (D-001810-10; Thermo Fisher Scientific) were used in loss-of-function experiments.

Cell proliferation, migration, and invasion assays. T24 and BOY cells were transfected with 10 nM miRNA or siRNA by reverse transfection. Cells were seeded in 96-well plates at 3×10^3 cells per well for XTT assays. After 72 h, cell proliferation was determined using a Cell Proliferation Kit II (Roche Diagnostics GmbH, Mannheim, Germany) as described previously (Tatarano *et al*, 2011; Kojima *et al*, 2012; Nohata *et al*, 2013). Cell migration activity was evaluated with wound healing assays. Cells were plated in 6-well plates at 2×10^5 cells per well, and after 48 h of transfection, the cell monolayer was scraped using a P-20 micropipette tip. The initial gap length (0 h) and the residual gap length 24 h after wounding were calculated from photomicrographs as described (Tatarano *et al*, 2011; Kojima *et al*, 2012; Nohata *et al*, 2013). Cell invasion assays were performed using modified Boyden chambers consisting of Transwell precoated Matrigel membrane filter inserts with 8-mm pores in 24-well tissue culture plates (BD Biosciences, Bedford, MA, USA). At 72 h after transfection, cells were plated in 24-well plates at 1×10^5 cells per well. Minimum essential medium containing 10% foetal bovine serum in the lower chamber served as the chemoattractant, as described previously (Tatarano *et al*, 2011; Kojima *et al*, 2012; Nohata *et al*, 2013). All experiments were performed in triplicate.

Western blot analysis. Cells were harvested 72 h after transfection, and lysates were prepared. Fifty micrograms of protein was separated by NuPAGE on 4–12% bis-tris gels (Invitrogen, Carlsbad, CA, USA) and transferred to PVDF membranes. Immunoblotting was carried out with diluted anti-PLOD2 antibodies (1 : 200; 21214-1-AP; Proteintech, Chicago, IL, USA) and anti-GAPDH antibodies (MAB374; Chemicon, Temecula, CA, USA). Specific complexes were visualised with an Echo-chemiluminescence Detection System (GE Healthcare, Little Chalfont, UK) as described previously (Yoshino *et al*, 2011; Kinoshita *et al*, 2013).

Genome-wide gene expression analysis and *in silico* analysis for the identification of genes regulated by *miR-26a-5p* and *miR-26b-5p*. *In silico* analysis was used to identify target genes of *miR-26a-5p* and *miR-26b-5p*. To obtain candidate target genes regulated by *miR-26a-5p* and *miR-26b-5p*, we used the TargetScan database Release 6.2 (http://www.targetscan.org). Additionally, the Gene Expression Omnibus database (accession numbers: GSE11783 and GSE31684) was used to identify upregulated genes in BC specimens.

Plasmid construction and dual-luciferase reporter assays. Partial wild-type sequences of the 3′-UTR of *PLOD2* or sequences with deletion of the *miR-26a-5p* and *miR-26b-5p* target sites (positions 905–912 and 1188–1194 of the *PLOD2* 3′-UTR) were inserted between the *Xho*I and *Pme*I restriction sites in the 3′-UTR of the *PLOD2* gene in the psiCHECK-2 vector (C8021; Promega, Madison, WI, USA). The protocol for vector construction was described previously (Chiyomaru *et al*, 2010; Kinoshita *et al*, 2013). The procedure for dual-luciferase reporter assay was described previously (Yoshino *et al*, 2013a).

Statistical analysis. The relationships between two groups were analysed using Mann–Whitney *U*-tests. The relationships between

three variables and numerical values were analysed using Bonferroni-adjusted Mann–Whitney *U*-tests. Overall survival (OS) in patients with BC was evaluated by the Kaplan–Meier method. Patients were divided into two groups according to the median value of *PLOD2* expression, and the differences between the two groups were evaluated by log-rank tests. Multivariable analysis was evaluated by the Cox proportional hazards model. All analyses were carried out using Expert StatView software, version 5.0 (SAS Institute, Cary, NC, USA).

RESULTS

Expression levels of *miR-26a-5p* and *miR-26b-5p* in BC. First, we evaluated the expression levels of *miR-26a-5p* and *miR-26b-5p* in BC tissues ($n=69$), and normal bladder epithelia ($n=23$). The expression levels of *miR-26a-5p* and *miR-26b-5p* were significantly reduced in tumour tissues compared with those in normal bladder epithelia ($P<0.0001$ and $P=0.0006$, respectively; Figure 1A). There were no significant relationships between any of the clinicopathological parameters (i.e., tumour stage, grade, and survival rate) and the expression levels of *miR-26a-5p* and *miR-26b-5p* (data not shown).

Effects of *miR-26a-5p and miR-26b-5p* restoration on cell proliferation, migration, and invasion activities in BC cell lines. We performed gain-of-function studies using *miR-26a-5p* or *miR-26b-5p* transfected T24 and BOY cells to investigate the functional roles of these miRNAs. XTT assays showed that *miR-26a-5p* and *miR-26b-5p* transfection inhibited cancer cell proliferation in BOY cells compared with that in mock or miR-control transfectants (Figure 1B). Moreover, migration assays demonstrated that cell migration activity was significantly inhibited in *miR-26a-5p* and *miR-26b-5p* transfectants in comparison with that in mock or miR-control transfectants (Figure 1B). Finally, Matrigel invasion assays demonstrated that cell invasion activity was significantly inhibited in *miR-26a-5p* and *miR-26b-5p* transfectants in comparison with that in mock or miR-control transfectants (Figure 1B). These data suggested that *miR-26a-5p* and *miR-26b-5p* functioned as tumour suppressors via inhibition of cell migration and invasion in BC.

Identification of molecular pathways modulated by *miR-26a/b* and putative target genes in BC cells. Next, *in silico* analysis was used to gain additional insights into the molecular mechanisms and pathways regulated by tumour-suppressive *miR-26a-5p* and *miR-26b-5p* in BC cells. Candidate *miR-26*-regulated genes were

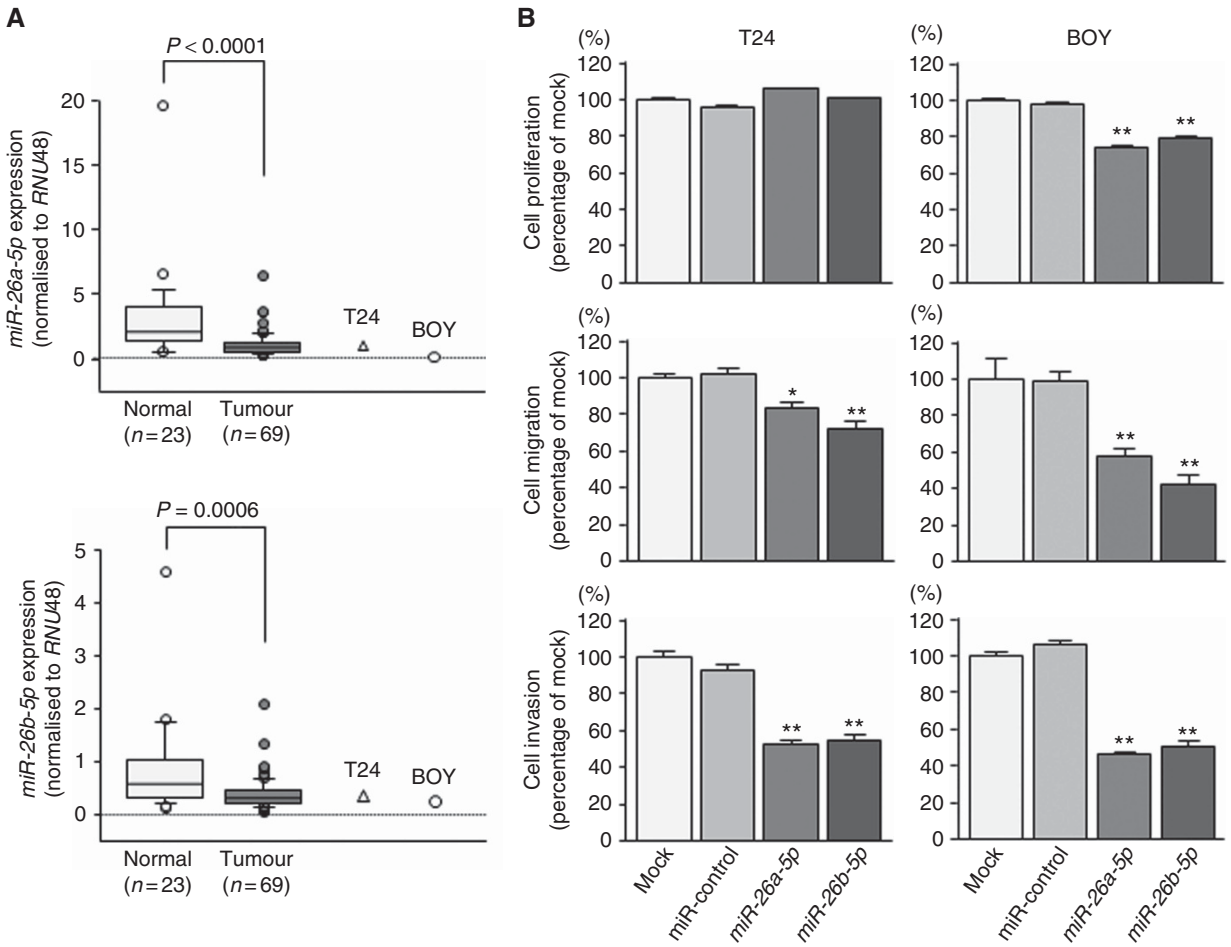

Figure 1. (**A**) Expression levels of *miR-26a-5p* and *miR-26b-5p*. Quantitative real-time reverse transcription–polymerase chain reaction showed that the expression levels of *miR-26a-5p* and *miR-26b-5p* were significantly lower in BC tissues and BC cell lines compared with that in non-BC tissues ($P<0.0001$ and $P=0.0006$, respectively). (**B**) Effects of *miR-26a-5p* and *miR-26b-5p* transfection on the functionality of BC cell lines. The XTT assay showed that cell proliferation was inhibited in *miR-26a-5p/26b-5p*-transfected BOY cells compared with that in mock or miR-control transfectants. However, cancer cell proliferation was not exhibited in *miR-26a-5p/26b-5p*-transfected T24 cells compared with that in mock or miR-control transfectants. Migration and invasion assays demonstrated that cell migration and invasion were significantly inhibited in *miR-26a-5p*- and *miR-26b-5p*-transfected cells in comparison with those in mock- or miR-control-transfected cells. *$P=0.002$; **$P<0.0001$.

identified using TargetScan database Release 6.2 (http://www.targetscan.org). Among these candidate genes, we selected 112 genes that had two or more conserved sites (Supplementary Table 2). We applied the Gene Expression Omnibus database (accession numbers: GSE11783 and GSE31684) to identify upregulated genes in BC specimens and subsequently selected the 28 genes listed in Table 1. For knockdown studies, it is necessary to select highly expressed genes. Evaluation of the expression levels of the top 6 genes in Table 1 by qRT–PCR showed that *LOXL2* and *PLOD2* were adequately expressed in the examined cell lines (Supplementary Figure 1). In this report, we have focused on *PLOD2*; studies of *LOXL2* are ongoing in our laboratory.

***PLOD2* was directly regulated by *miR-26a-5p* and *miR-26b-5p* in BC cells.** We performed qRT–PCR analysis and western blot analyses to confirm that restoration of *miR-26a-5p* and *miR-26b-5p* resulted in downregulation of *PLOD2* in T24 and BOY cells. *PLOD2* mRNA and protein levels were significantly reduced in *miR-26a-5p* and *miR-26b-5p* transfectants in comparison with those in mock or miR-control transfectants (Figure 2A).

We then performed dual-luciferase reporter assays in T24 and BOY cells to determine whether *PLOD2* was directly regulated by these miRNAs. The TargetScan database predicted that there were two binding sites for *miR-26a-5p* and *miR-26b-5p*

Table 1. Putative candidate of target genes

				TargetScan		Gene expression omnibus (GSE11783 + GSE31684)	
Entrez gene ID	Gene symbol	Description	Genomic location	Number of conserved sites	Number of poorly conserved sites	Fold change	*P*-value
647309	*GEMC1*	*Geminin coiled-coil domain-containing protein 1*	3q28	2	0	10.139	9.420E – 05
3759	*KCNJ2*	*Potassium inwardly rectifying channel, subfamily J, member 2*	17q24.3	2	0	6.435	5.670E – 05
4017	*LOXL2*	*Lysyl oxidase-like 2*	8p21.3	2	0	4.706	5.316E – 05
5352	*PLOD2*	*Procollagen-lysine, 2-oxoglutarate 5-dioxygenase 2*	3q24	2	0	4.616	1.135E – 04
170692	*ADAMTS18*	*ADAM metallopeptidase with thrombospondin type 1 motif, 18*	16q23	2	0	4.186	4.376E – 05
55117	*SLC6A15*	*Solute carrier family 6 (neutral amino-acid transporter), member 15*	12q21.3	2	0	4.119	1.640E – 04
144455	*E2F7*	*E2F transcription factor 7*	12q21.2	2	0	3.726	5.316E – 05
23657	*SLC7A11*	*Solute carrier family 7 (anionic amino-acid transporter light chain, xc system), member 11*	4q28.3	2	2	3.381	1.003E – 04
84206	*MEX3B*	*Mex-3 homologue B (Caenorhabditis elegans)*	15q25.2	2	0	3.293	9.231E – 03
1993	*ELAVL2*	*ELAV (embryonic lethal, abnormal vision, Drosophila)-like 2 (Hu antigen B)*	9p21	3	0	3.237	7.790E – 04
10847	*SRCAP*	*Snf2-related CREBBP activator protein*	16p11.2	2	0	2.818	8.308E – 05
7468	*WHSC1*	*Wolf–Hirschhorn syndrome candidate 1*	4p16.3	2	0	2.590	4.670E – 05
9120	*SLC16A6*	*Solute carrier family 16, member 6 (monocarboxylic acid transporter 7)*	17q24.2	2	0	2.431	1.285E – 04
54620	*FBXL19*	*F-box and leucine-rich repeat protein 19*	16p11.2	2	0	2.429	1.405E – 03
10622	*POLR3G*	*Polymerase (RNA) III (DNA directed) polypeptide G (32 kDa)*	5q14.3	2	2	2.281	1.642E – 03
64768	*IPPK*	*Inositol 1,3,4,5,6-pentakisphosphate 2-kinase*	9q22.31	2	0	2.223	1.067E – 04
23276	*KLHL18*	*Kelch-like 18 (Drosophila)*	3p21.31	2	1	1.854	4.670E – 05
124801	*LSM12*	*LSM12 homologue (Saccharomyces cerevisiae)*	17q21.31	2	0	1.795	1.003E – 04
54726	*OTUD4*	*OTU domain containing 4*	4q31.21	2	1	1.589	2.975E – 04
2182	*ACSL4*	*Acyl-CoA synthetase long-chain family member 4*	Xq22.3-q23	2	0	1.589	8.447E – 03
51701	*NLK*	*Nemo-like kinase*	17q11.2	2	1	1.548	1.405E – 03
200424	*TET3*	*Tet oncogene family member 3*	2p13.1	3	1	1.456	1.421E – 02
26973	*CHORDC1*	*Cysteine and histidine-rich domain (CHORD) containing 1*	11q14.3	2	1	1.435	7.383E – 03
23633	*KPNA6*	*Karyopherin α6 (importin α7)*	1p35.1	2	1	1.413	7.373E – 04
85403	*EAF1*	*ELL-associated factor 1*	3p25.1	2	1	1.372	1.148Ev02
27	*ABL2*	*v-abl Abelson murine leukaemia viral oncogene homologue 2*	1q25.2	3	2	1.371	3.487E – 03
23367	*LARP1*	*La ribonucleoprotein domain family, member 1*	5q33.2	2	1	1.299	2.057E – 02
114885	*OSBPL11*	*Oxysterol binding protein-like 11*	3q21	2	0	1.289	1.749E – 02

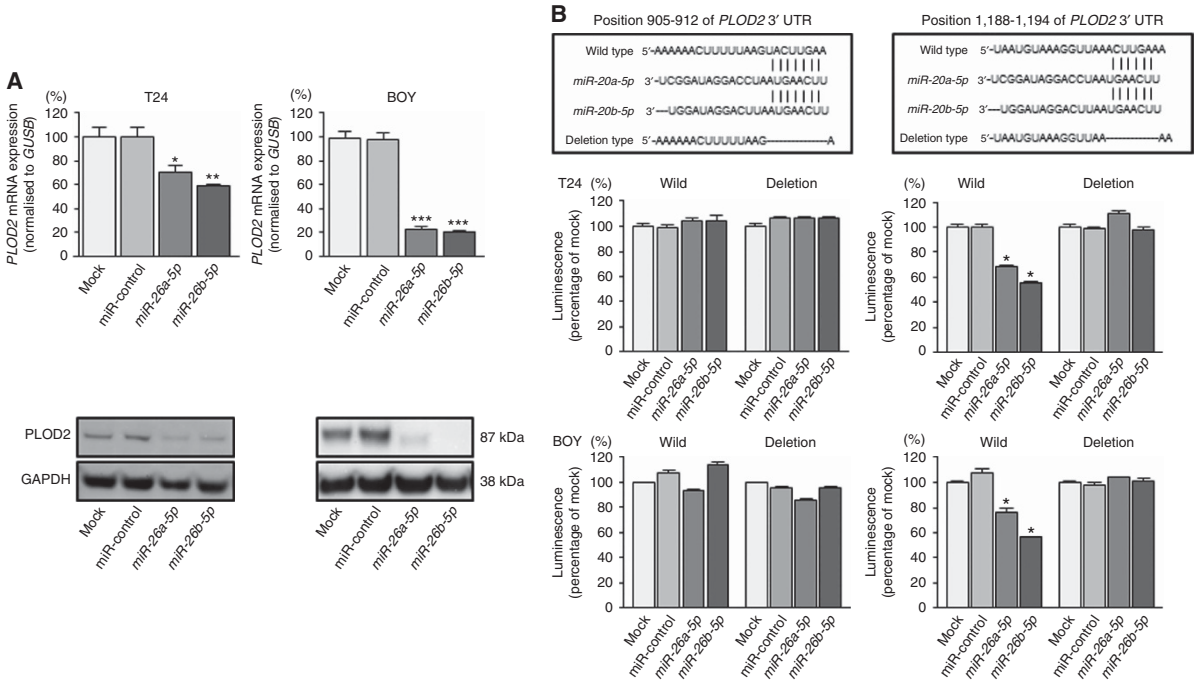

Figure 2. Direct regulation of *PLOD2* by *miR-26a-5p* and *miR-26b-5p*. (**A**) The expression of *PLOD2* was significantly repressed in *miR-26a-5p/26b-5p* transfectants in comparison with that in mock or miR-control transfectants. *GUSB* was used as an internal control. $*P=0.0109$; $**P=0.0016$; $***P<0.0001$. The expression of PLOD2 protein was significantly repressed in *miR-26a-5p/26b-5p* transfectants in comparison with that in mock or miR-control transfectants. *GAPDH* was used for a loading control. (**B**) *miR-26a-5p/26b-5p* binding sites at positions 1188–1194 in the 3′-UTR of *PLOD2* mRNA. Dual-luciferase reporter assays using vectors encoding putative *miR-26a-5p/26b-5p* target sites for wild-type or deleted regions. Normalised data were calculated as ratios of *Renilla*/firefly luciferase activities. The luminescence intensity was significantly reduced by co-transfection with *miR-26a-5p/26b-5p* and the vector carrying the wild-type sequence for positions 1188–1194 in the 3′-UTR of *PLOD2* mRNA, whereas transfection with the deletion vector and the wild-type sequence for positions 905–912 in the 3′-UTR of *PLOD2* mRNA blocked the decrease in luminescence. $*P<0.0001$.

at positions 905–912 and 1188–1194 in the *PLOD2* 3′-UTR. We used vectors encoding the partial wild-type sequence of the 3′-UTR of *PLOD2*, including the predicted *miR-26a-5p*/*miR-26b-5p* target sites. We found that the luminescence intensity was significantly reduced by co-transfection with *miR-26a-5p* or *miR-26b-5p* and the vector carrying the wild-type sequences at positions 1188–1194 of the *PLOD2* 3′-UTR, whereas transfection with the deletion vector (in which the binding site had been removed) and the wild-type sequence at positions 905–912 of the *PLOD2* 3′-UTR blocked the decrease in luminescence (Figure 2B). These data suggested that *miR-26a-5p*/*26b-5p* bound directly to specific sites at positions 1188–1194 of the *PLOD2* 3′-UTR.

Effects of *PLOD2* knockdown on cell proliferation, migration, and invasion in BC cell lines. To investigate the functional role of *PLOD2* in BC cells, we performed loss-of-function studies using cells transfected with two *si-PLOD2* constructs (*si-PLOD2*-1 and *si-PLOD2*-2). We evaluated the knockdown efficiency of *si-PLOD2* transfection in T24 and BOY cells. Quantitative real-time reverse transcription–polymerase chain reaction analysis and western blot analysis indicated that these siRNAs effectively downregulated *PLOD2* mRNA and protein expression in both cell lines (Figure 3A). XTT assays demonstrated that cell proliferation was not inhibited in *si-PLOD2* transfectants in comparison with that in mock or miR-control transfectants (Figure 3B). In contrast, migration assays demonstrated that cell migration activity was significantly inhibited in *si-PLOD2* transfectants in comparison with that in mock or miR-control transfectants (Figure 3B). Matrigel invasion assays demonstrated that cell invasion activity was significantly inhibited in *si-PLOD2* transfectants in comparison with that in mock or miR-control transfectants (Figure 3B).

Expression levels of *PLOD2* in BC specimens. Quantitative real-time reverse transcription–polymerase chain reaction analysis showed that *PLOD2* expression was significantly upregulated in BC specimens ($n=69$) compared with that in normal specimens ($n=23$; $P<0.0001$; Figure 4A). Spearman's rank test showed the trend towards significance about inverse correlations between the expression levels of *miR-26a-5p*/*miR-26b-5p* and *PLOD2* ($P=0.1248$, $R=-0.159$ and $P=0.1345$, $R=-0.155$, respectively; Figure 4B). The expression level of *PLOD2* was significantly higher in pT3 and pT4 specimens ($P=0.0119$) and in BCs with positive lymph node invasion ($P=0.0490$) compared with that in their counterparts (Figure 4C). However, we could not find the positive correlations in terms of other clinicopathological parameters (Supplementary Figure 2). Moreover, Kaplan–Meier analysis showed that patients in the high *PLOD2* expression group exhibited significantly shorter OS than patients in the low *PLOD2* expression group ($P=0.0153$; Figure 4D). When we looked at the muscle-invasive cancer group, there was a trend towards significance between PLOD2 and survival ($P=0.0571$). Our cohort might be too small to find a positive correlations in the muscle-invasive cancer groups. There was also a trend towards significance of *PLOD2* expression with OS after controlling for pathologic stage, age, and gender in a multivariable analysis ($P=0.0545$) (Supplementary Table 4).

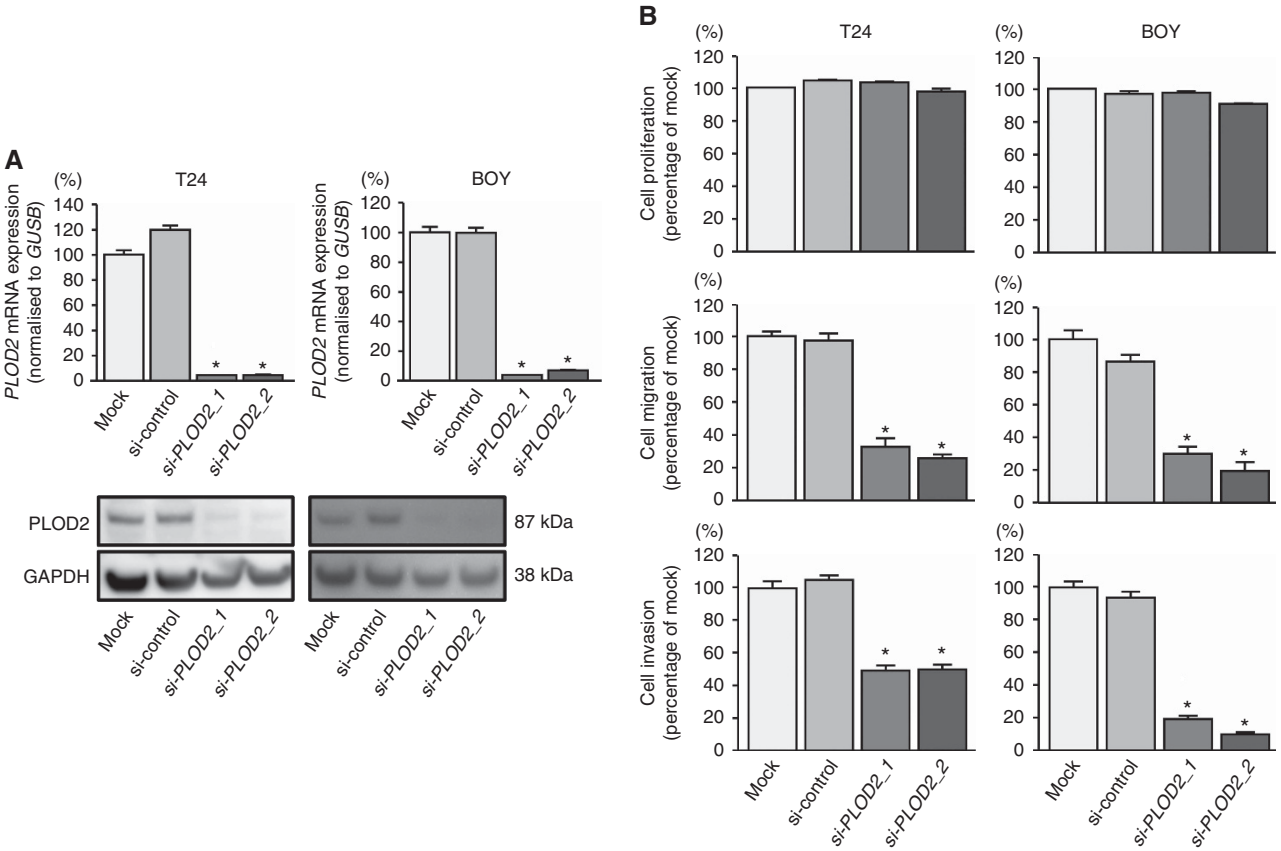

Figure 3. Effects of *si-PLOD2* transfection on BC cell lines. We evaluated the knockdown efficiency of *si-PLOD2*-1 and *si-PLOD2*-2 transfection in T24 and BOY cells. (**A**) Quantitative real-time reverse transcription–polymerase chain reaction analysis indicated that these siRNAs effectively downregulated *PLOD2* expression in both cell lines. *$P<0.0001$. Western blot analyses indicated that these siRNAs effectively downregulated PLOD2 protein expression in both cell lines. (**B**) XTT assays demonstrated that cell proliferation was not inhibited in *si-PLOD2*-transfected cells in comparison with that in mock- or miR-control-transfected cells. Migration and Matrigel invasion assays demonstrated that cell migration and invasion were significantly inhibited in *si-PLOD2*-transfected cells in comparison with that in mock- or miR-control-transfected cells. *$P<0.0001$.

DISCUSSION

Although many studies have shown that miRNA regulatory mechanisms can be disrupted by the aberrant expression of tumour-suppressive or oncogenic miRNAs in cancer cells, each miRNA targets different genes and cancer pathways. Therefore, identification of tumour-suppressive miRNAs and the molecular pathways mediated by these miRNAs is important to improve our understanding of cancer mechanisms. We have previously reported that tumour-suppressive miRNAs mediate novel molecular targets and pathways in some types of cancers (Yoshino *et al*, 2013b; Matsushita *et al*, 2015). Among them, we found that some miRNAs contribute to BC development, progression, and metastasis (Yoshino *et al*, 2013c).

In this study, we focused on *miR-26a/b* because these miRNAs have been shown to have strong anticancer effects in prostate cancer, head and neck carcinoma, and papillary thyroid carcinoma (Fukumoto *et al*, 2015; Kato *et al*, 2015; You *et al*, 2015) through regulation of genes associated with the ECM and cell cycle regulation. Other researchers have also reported that *miR-26a* delivery prevents the progression of hepatocellular carcinoma, highlighting its potential therapeutic applications (Kota *et al*, 2009). In addition, *c-MYC* has been reported to suppress *miR-26a* and *miR-26b* (Chang *et al*, 2008). Because *miR-26a-5p* and *miR-26b-5p* may regulate different molecular targets in several cancers, elucidation of the molecular mechanisms of aberrant *miR-26a-5p* and *miR-26b-5p* expression in each type of cancer is important. In our study, these miRNAs were significantly downregulated in clinical BC specimens compared with those in normal bladder tissue, suggesting that these miRNAs may function as tumour suppressors in BC. Moreover, cell function assays revealed that cell migration and invasion were inhibited in BC cells transfected with these miRNAs.

During our *miR-26a/b* target analyses, we used *in silico* analysis with the TargetScan database to obtain candidate *miR-26*-regulated genes. Among these candidate genes, we identified 112 genes having two or more conserved sites. In addition, we applied the Gene Expression Omnibus database to identify upregulated genes in BC clinical specimens. From this analysis, we selected 28 genes for further analysis. Molecular target searches suggested that *PLOD2*, a collagen crosslinking enzyme, was a promising candidate target regulated by these miRNAs in BC cells.

PLOD2 is a collagen-modifying enzyme, similar to prolyl 4-hydroxylase α-subunit (P4HA) isoform 1, P4HA2, and LOX. Procollagens are post-translationally modified within the cisternae of the endoplasmic reticulum by P4HA1–3 and PLOD1-3 lysyl hydroxylase enzymes. Collagen, similar to elastics, fibronectins, laminins, and proteoglycans, is an ECM protein that regulates tissue homeostasis, organ development, inflammation, and diseases such as cancer. Therefore, aberrant expression of *PLOD2* results in

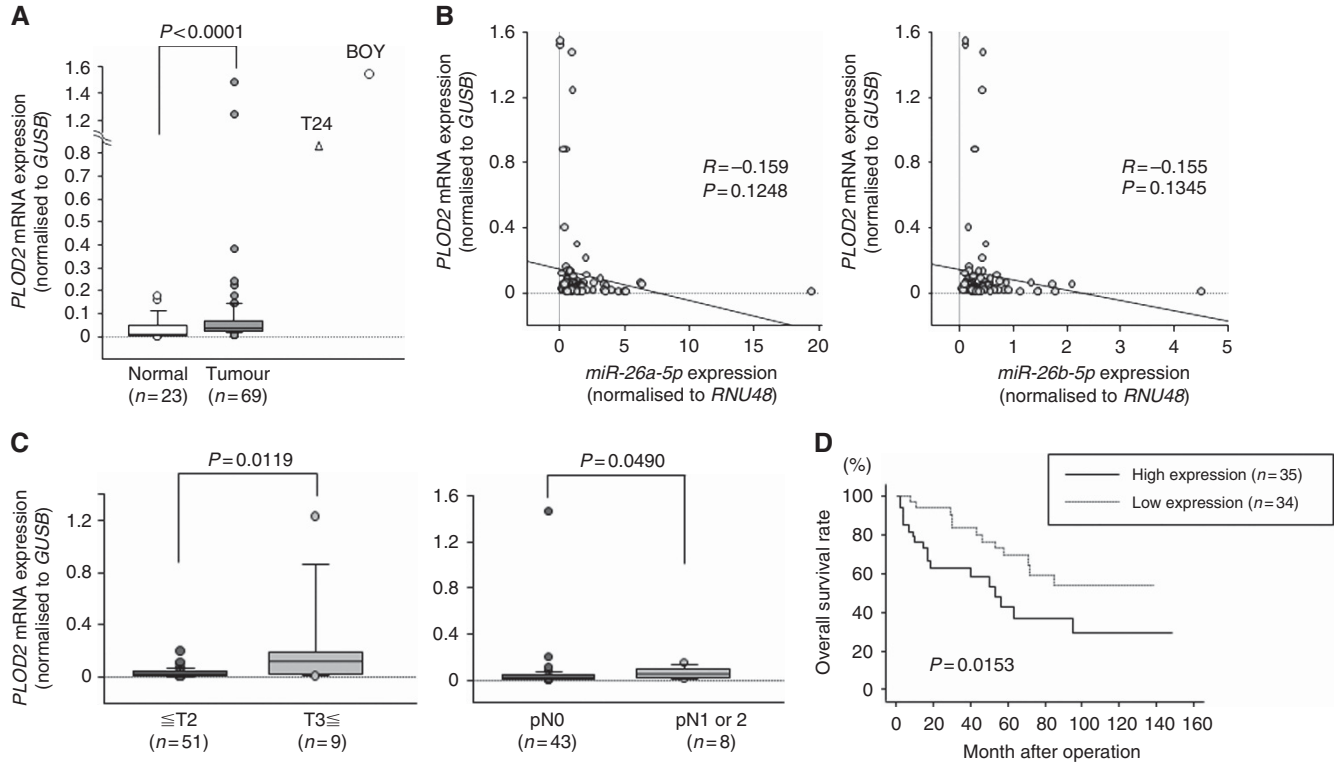

Figure 4. Expression level of *PLOD2* in BC clinical specimens. (**A**) The expression level of *PLOD2* was significantly upregulated in BC tissues in comparison with that in normal bladder tissues. *GUSB* was used for normalisation ($P=0.0001$). (**B**) Spearman's rank test showed the trend towards significance about inverse correlations between the expression levels of *miR-26a-5p/miR-26b-5p* and *PLOD2* ($P=0.1248$, $R=-0.159$ and $P=0.1345$, $R=-0.155$, respectively). (**C**) To determine whether the levels of *PLOD2* mRNA in tumour tissues were correlated with clinicopathological parameters, we analysed the expression level of the *PLOD2* gene in human tumour samples. *PLOD2* expression was significantly increased in samples from patients with T3 stage disease as compared with that in samples from patients with T2 stage disease or lower ($P=0.0119$). Additionally, *PLOD2* expression was significantly increased in pN1 or pN2 samples compared with that in pN0 samples ($P=0.0490$). (**D**) Kaplan–Meier survival plots for high and low expression groups for *PLOD2*, as determined for 69 patients. Overall survival was significantly prolonged in patients with low *PLOD2* expression compared with that in patients with high expression ($P=0.0153$). The median follow-up of the patients was 45.8 months.

ECM disruption, promoting cell migration and invasion. A recent study showed that high expression of *PLOD2* mRNA in breast cancer was associated with poorer disease-free survival of 159 patients (Gilkes *et al*, 2013). Another report in breast cancer showed that the expression levels of *miR-26a* and *miR-26b* are decreased by oestrogen stimulation and that forced expression of *miR-26a* or *miR-26b* negatively regulates oestrogen-stimulated breast cancer cell growth both *in vitro* and *in vivo*. Additionally, oestrogen-dependent *c-MYC* expression suppresses *miR-26a* and *miR-26b* expression. Interestingly, screening of oestrogen-responsive genes predicted to be targeted by *miR-26* led to identification of *PLOD2* and other targets (Tan *et al*, 2014). In our study, *PLOD2* knockdown BC cells inhibited cell migration and invasion. Importantly, high expression of *PLOD2* was associated with poorer OS. Therefore, we speculated that *miR-26a/b* downregulation triggered upregulation of *PLOD2*, contributing to the poor outcomes observed in patients with BC. However, despite the observed correlations between *PLOD2* and survival, our data did not show any correlations between *miR-26* and survival. In our speculation, this observation may be explained by the fact that multiple microRNAs would target *PLOD2*. Therefore, it is no wonder that no correlations were found between individual miRNAs and the survival in BC patients. We also could not find any correlations between *PLOD2* mRNA expression and the recurrence status in the BC patients (Supplementary Figure 2). Our cohort included patients who had undergone different treatment modalities such as radical cystectomy or TURBT with or without adjuvant bacillus calmette guerin instillation into bladder. Thus, these complicated background may affect the results.

Furthermore, we investigated the molecular mechanisms of *PLOD2* downstream signalling using *si-PLOD2* transfectants, as shown in Table 2. Our results showed that hexokinase 2 (*HK2*) was a potential target of *PLOD2* signalling in BC cells (Supplementary Table 3). In rapidly growing tumour tissue, hypoxia-inducible factor (HIF)-1 helps hypoxic tumour cells to shift toward the glycolytic pathway from the more efficient oxidative phosphorylation pathway to maintain energy production (the Warburg effect). Therefore, hypoxic cells tend to consume more glucose to meet their energy needs. Hypoxia-inducible factor 1 mediates this metabolic conversion through the induction of enzymes involved in the glycolysis pathway, such as *HK2* and glucose transporters (Masoud and Li, 2015). Among these, our recent study showed that the tumour-suppressive *miR-143/145* cluster directly regulates *HK2* in renal cell carcinoma cells (Yoshino *et al*, 2013a). Although we did not demonstrate a correlation between hypoxia and *miR-26a/b* or *PLOD2* in this study, it is plausible that hypoxia might inhibit *miR-26a/b*, leading to increased expression of *PLOD2* and *HK2*. Therefore, further studies are necessary.

Investigation of the molecular mechanisms downstream of *PLOD2* signalling also identified integrin A3 (*ITGA3*). Integrins comprise a large family of cell receptors for ECM proteins and ligands, such as fibronectin and collagen on other cells. Therefore,

Table 2. Significantly enriched pathways (downstream genes of *PLOD2*)

KEGG pathway entry number	Annotation	Number of genes	*P*-value	Genes								
4010	MAPK signalling pathway	16	8.14E – 04	*IL1B*	*GADD45A*	*FGF2*	*DDIT3*	*FLNA*	*IL1A*	*DUSP6*	*DUSP5*	*MECOM*
				CASP3	*KRAS*	*RPS6KA3*	*ARRB1*	*GADD45B*	*PAK2*	*DUSP22*		
5200	Pathways in cancer	14	1.56E – 02	*CYCS*	*FGF2*	*ITGA6*	*ITGA3*	*TPM3*	*TCEB1*	*LAMC1*	*MECOM*	*CASP3*
				WNT5B	*KRAS*	*RALA*	*TRAF1*	*CBLB*				
4141	Protein processing in endoplasmic reticulum	14	8.33E – 05	*UBE2J1*	*HYOU1*	*HSPA5*	*DNAJA2*	*DNAJB11*	*DDIT3*	*UBE2E1*	*DNAJC1*	*SEC24A*
				DERL2	*MAN1A2*	*CAPN2*	*HERPUD1*	*PDIA4*				
4144	Endocytosis	9	3.67E – 02	*ITCH*	*CAV1*	*PIP5KL1*	*RAB31*	*SMAP2*	*ARRB1*	*EPS15*	*ERBB3*	*CBLB*
5152	Tuberculosis	9	2.53E – 02	*IL1B*	*CYCS*	*RIPK2*	*CREB1*	*IL1A*	*CASP3*	*CEBPG*	*CORO1A*	*HLA-DMB*
4120	Ubiquitin-mediated proteolysis	9	7.81E – 03	*CDC26*	*UBE2J1*	*PRPF19*	*CDC20*	*ITCH*	*UBE2E1*	*TCEB1*	*ERCC8*	*CBLB*
4910	Insulin signalling pathway	9	7.78E – 03	*EXOC7*	*HK2*	*RPS6KB1*	*RHEB*	*HKDC1*	*KRAS*	*PPP1R3C*	*PYGL*	*CBLB*
5010	Alzheimer's disease	8	4.15E – 02	*IL1B*	*CYCS*	*APH1A*	*CAPN2*	*NDUFB3*	*PLCB3*	*CASP3*	*COX7A2L*	
5323	Rheumatoid arthritis	8	1.75E – 03	*IL1B*	*ATP6V1C1*	*ATP6V1A*	*CCL20*	*IL1A*	*CSF1*	*CCL5*	*HLA-DMB*	
3008	Ribosome biogenesis in eukaryotes	8	8.44E – 04	*UTP18*	*NOL6*	*NOP56*	*NXT1*	*DKC1*	*WDR43*	*UTP14A*	*RPP40*	
4115	p53 signalling pathway	8	6.70E – 04	*CYCS*	*GADD45A*	*SESN2*	*CASP3*	*STEAP3*	*CCNG1*	*GADD45B*	*PMAIP1*	
4110	Cell cycle	7	3.68E – 02	*CDC26*	*GADD45A*	*CDC20*	*CDC25C*	*MAD2L1*	*ORC1*	*GADD45B*		
4012	ErbB signalling pathway	7	9.20E – 03	*NRG1*	*RPS6KB1*	*NRG2*	*KRAS*	*PAK2*	*ERBB3*	*CBLB*		
4640	Haematopoietic cell lineage	7	7.55E – 03	*IL1B*	*ITGA6*	*ITGA3*	*IL1A*	*CSF1*	*CD9*	*IL7*		
520	Amino sugar and nucleotide sugar metabolism	7	8.07E – 04	*HK2*	*UAP1*	*UGDH*	*GNPNAT1*	*GNPDA1*	*HKDC1*	*GFPT1*		
970	Aminoacyl-tRNA biosynthesis	6	1.23E – 03	*IARS*	*FBXO17*	*GARS*	*MTFMT*	*YARS*	*SARS*			
5020	Prion diseases	6	6.56E – 04	*IL1B*	*HSPA5*	*IL1A*	*LAMC1*	*PRNP*	*CCL5*			
5120	Epithelial cell signaling in *Helicobacter pylori* infection	5	3.82E – 02	*JAM2*	*ATP6V1C1*	*ATP6V1A*	*CASP3*	*CCL5*				
3018	RNA degradation	5	3.74E – 02	*DCPS*	*PAN3*	*ENO3*	*CNOT6*	*LSM5*				
5416	Viral myocarditis	5	3.35E – 02	*CYCS*	*CAV1*	*CASP3*	*EIF4G2*	*HLA-DMB*				
10	Glycolysis/ gluconeogenesis	5	3.29E – 02	*HK2*	*ENO3*	*HKDC1*	*PGAM1*	*PGAM4*				
4150	mTOR signalling pathway	5	2.01E – 02	*RPS6KB1*	*RHEB*	*EIF4B*	*CAB39L*	*RPS6KA3*				
500	Starch and sucrose metabolism	5	1.98E – 02	*HK2*	*ENPP1*	*UGDH*	*HKDC1*	*PYGL*				
4130	SNARE interactions in vesicular transport	4	2.60E – 02	*VAMP1*	*VAMP4*	*STX3*	*BET1*					
260	Glycine, serine and threonine metabolism	4	2.09E – 02	*CTH*	*PHGDH*	*PSAT1*	*PSPH*					
910	Nitrogen metabolism	3	4.18E – 02	*ASNS*	*CTH*	*CA13*						
524	Butirosin and neomycin biosynthesis	2	2.52E – 02	*HK2*	*HKDC1*							

Abbreviations: KEGG = Kyoto Encyclopedia of Genes and Genomes; MAPK = mitogen-activated protein kinase; mTOR = mammalian target of rapamycin; PLOD2 = procollagen-lysine, 2-oxoglutarate 5-dioxygenase 2; SNARE = soluble *N*-ethylmaleimide-sensitive factor attached protein receptor.

aberrant expression of extracellular proteins triggers intracellular signalling events, which may lead to cancer metastasis and invasion (Givant-Horwitz *et al*, 2005). Based on our study, *PLOD2*-induced ECM fibrosis may contribute to aberrant intracellular signalling. Our recent study showed that the tumour-suppressive *miR-223* directly regulates *ITGA3*/*ITGB1* in prostate cancer (Kurozumi *et al*, 2016), suggesting that *miR-26a*/*b* may also regulate *ITGA3* through *PLOD2* regulation in BC. Because there is no evidence of direct connections among *PLOD2*, *HK2*, and integrin, further studies are necessary.

CONCLUSIONS

Downregulation of *miR-26a-5p* and *miR-26b-5p* was frequently observed in BC cells, and both of these miRNAs significantly inhibited cancer cell migration and invasion. *PLOD2* was directly regulated by the tumour suppressors *miR-26a-5p* and *miR-26b-5p* and may be a good prognostic marker for survival in patients with BC. Recent studies have shown that aberrant expression of ECM components contributes to cancer cell invasion and metastasis. *PLOD2* functions as a collagen crosslinking enzyme is associated with ECM stiffness. This is the first report demonstrating the positive correlation between *PLOD2* and survival in clinical BC specimens. The discovery of molecular targets mediated by tumour-suppressive miRNAs provides important insights into the potential mechanisms of BC metastasis.

ACKNOWLEDGEMENTS

This study was supported by the KAKENHI (C), 25462490.

CONFLICT OF INTEREST

The authors declare no conflict of interest.

REFERENCES

Bartel DP (2004) MicroRNAs: genomics, biogenesis, mechanism, and function. *Cell* **116**: 281–297.

Bellmunt J, Petrylak DP (2012) New therapeutic challenges in advanced bladder cancer. *Semin Oncol* **39**: 598–607.

Carthew RW, Sontheimer EJ (2009) Origins and mechanisms of miRNAs and siRNAs. *Cell* **136**: 642–655.

Chang TC, Yu D, Lee YS, Wentzel EA, Arking DE, West KM, Dang CV, Thomas-Tikhonenko A, Mendell JT (2008) Widespread microRNA repression by Myc contributes to tumorigenesis. *Nat Genet* **40**: 43–50.

Chiyomaru T, Enokida H, Tatarano S, Kawahara K, Uchida Y, Nishiyama K, Fujimura L, Kikkawa N, Seki N, Nakagawa M (2010) miR-145 and miR-133a function as tumour suppressors and directly regulate FSCN1 expression in bladder cancer. *Br J Cancer* **102**: 883–891.

De Santis M, Bellmunt J, Mead G, Kerst JM, Leahy M, Maroto P, Gil T, Marreaud S, Daugaard G, Skoneczna I, Collette S, Lorent J, de Wit R, Sylvester R (2012) Randomized phase II/III trial assessing gemcitabine/carboplatin and methotrexate/carboplatin/vinblastine in patients with advanced urothelial cancer who are unfit for cisplatin-based chemotherapy: EORTC study 30986. *J Clin Oncol* **30**: 191–199.

Di Leva G, Croce CM (2010) Roles of small RNAs in tumor formation. *Trends Mol Med* **16**: 257–267.

Fukumoto I, Hanazawa T, Kinoshita T, Kikkawa N, Koshizuka K, Goto Y, Nishikawa R, Chiyomaru T, Enokida H, Nakagawa M, Okamoto Y, Seki N (2015) MicroRNA expression signature of oral squamous cell carcinoma: functional role of microRNA-26a/b in the modulation of novel cancer pathways. *Br J Cancer* **112**: 891–900.

Ghosh M, Brancato SJ, Agarwal PK, Apolo AB (2014) Targeted therapies in urothelial carcinoma. *Curr Opin Oncol* **26**: 305–320.

Gilkes DM, Bajpai S, Wong CC, Chaturvedi P, Hubbi ME, Wirtz D, Semenza GL (2013) Procollagen lysyl hydroxylase 2 is essential for hypoxia-induced breast cancer metastasis. *Mol Cancer Res* **11**: 456–466.

Gilkes DM, Semenza GL, Wirtz D (2014) Hypoxia and the extracellular matrix: drivers of tumour metastasis. *Nat Rev Cancer* **14**: 430–439.

Givant-Horwitz V, Davidson B, Reich R (2005) Laminin-induced signaling in tumor cells. *Cancer Lett* **223**: 1–10.

Ichimi T, Enokida H, Okuno Y, Kunimoto R, Chiyomaru T, Kawamoto K, Kawahara K, Toki K, Kawakami K, Nishiyama K, Tsujimoto G, Nakagawa M, Seki N (2009) Identification of novel microRNA targets based on microRNA signatures in bladder cancer. *Int J Cancer* **125**: 345–352.

Inoguchi S, Seki N, Chiyomaru T, Ishihara T, Matsushita R, Mataki H, Itesako T, Tatarano S, Yoshino H, Goto Y, Nishikawa R, Nakagawa M, Enokida H (2014) Tumour-suppressive microRNA-24-1 inhibits cancer cell proliferation through targeting FOXM1 in bladder cancer. *FEBS Lett* **588**: 3170–3179.

Itesako T, Seki N, Yoshino H, Chiyomaru T, Yamasaki T, Hidaka H, Yonezawa T, Nohata N, Kinoshita T, Nakagawa M, Enokida H (2014) The microRNA expression signature of bladder cancer by deep sequencing: the functional significance of the miR-195/497 cluster. *PLoS One* **9**: e84311.

Kato M, Goto Y, Matsushita R, Kurozumi A, Fukumoto I, Nishikawa R, Sakamoto S, Enokida H, Nakagawa M, Ichikawa T, Seki N (2015) MicroRNA-26a/b directly regulate La-related protein 1 and inhibit cancer cell invasion in prostate cancer. *Int J Oncol* **47**: 710–718.

Kinoshita T, Nohata N, Hanazawa T, Kikkawa N, Yamamoto N, Yoshino H, Itesako T, Enokida H, Nakagawa M, Okamoto Y, Seki N (2013) Tumour-suppressive microRNA-29s inhibit cancer cell migration and invasion by targeting laminin-integrin signalling in head and neck squamous cell carcinoma. *Br J Cancer* **109**: 2636–2645.

Kojima S, Chiyomaru T, Kawakami K, Yoshino H, Enokida H, Nohata N, Fuse M, Ichikawa T, Naya Y, Nakagawa M, Seki N (2012) Tumour suppressors miR-1 and miR-133a target the oncogenic function of purine nucleoside phosphorylase (PNP) in prostate cancer. *Br J Cancer* **106**: 405–413.

Kota J, Chivukula RR, O'Donnell KA, Wentzel EA, Montgomery CL, Hwang HW, Chang TC, Vivekanandan P, Torbenson M, Clark KR, Mendell JR, Mendell JT (2009) Therapeutic microRNA delivery suppresses tumorigenesis in a murine liver cancer model. *Cell* **137**: 1005–1017.

Kurozumi A, Goto Y, Matsushita R, Fukumoto I, Kato M, Nishikawa R, Sakamoto S, Enokida H, Nakagawa M, Ichikawa T, Seki N (2016) Tumor-suppressive microRNA-223 inhibits cancer cell migration and invasion by targeting ITGA3/ITGB1 signaling in prostate cancer. *Cancer Sci* **107**: 84–94.

Masoud GN, Li W (2015) HIF-1alpha pathway: role, regulation and intervention for cancer therapy. *Acta Pharm Sin B* **5**: 378–389.

Matsushita R, Seki N, Chiyomaru T, Inoguchi S, Ishihara T, Goto Y, Nishikawa R, Mataki H, Tatarano S, Itesako T, Nakagawa M, Enokida H (2015) Tumour-suppressive microRNA-144-5p directly targets CCNE1/2 as potential prognostic markers in bladder cancer. *Br J Cancer* **113**: 282–289.

Meeks JJ, Bellmunt J, Bochner BH, Clarke NW, Daneshmand S, Galsky MD, Hahn NM, Lerner SP, Mason M, Powles T, Sternberg CN, Sonpavde G (2012) A systematic review of neoadjuvant and adjuvant chemotherapy for muscle-invasive bladder cancer. *Eur Urol* **62**: 523–533.

Nohata N, Hanazawa T, Kinoshita T, Inamine A, Kikkawa N, Itesako T, Yoshino H, Enokida H, Nakagawa M, Okamoto Y, Seki N (2013) Tumour-suppressive microRNA-874 contributes to cell proliferation through targeting of histone deacetylase 1 in head and neck squamous cell carcinoma. *Br J Cancer* **108**: 1648–1658.

Siegel R, Naishadham D, Jemal A (2012) Cancer statistics, 2012. *CA Cancer J Clin* **62**: 10–29.

Sobin LH, Compton CC (2010) TNM seventh edition: what's new, what's changed: communication from the International Union Against Cancer and the American Joint Committee on Cancer. *Cancer* **116**: 5336–5339.

Tan S, Ding K, Li R, Zhang W, Li G, Kong X, Qian P, Lobie PE, Zhu T (2014) Identification of miR-26 as a key mediator of estrogen stimulated cell proliferation by targeting CHD1, GREB1 and KPNA2. *Breast Cancer Res* **16**: R40.

Tatarano S, Chiyomaru T, Kawakami K, Enokida H, Yoshino H, Hidaka H, Yamasaki T, Kawahara K, Nishiyama K, Seki N, Nakagawa M (2011) miR-218 on the genomic loss region of chromosome 4p15.31 functions as a tumor suppressor in bladder cancer. *Int J Oncol* **39**: 13–21.

Yoshino H, Chiyomaru T, Enokida H, Kawakami K, Tatarano S, Nishiyama K, Nohata N, Seki N, Nakagawa M (2011) The tumour-suppressive function of miR-1 and miR-133a targeting TAGLN2 in bladder cancer. *Br J Cancer* **104**: 808–818.

Yoshino H, Enokida H, Itesako T, Kojima S, Kinoshita T, Tatarano S, Chiyomaru T, Nakagawa M, Seki N (2013a) Tumor-suppressive

microRNA-143/145 cluster targets hexokinase-2 in renal cell carcinoma. *Cancer Sci* **104**: 1567–1574.

Yoshino H, Enokida H, Itesako T, Tatarano S, Kinoshita T, Fuse M, Kojima S, Nakagawa M, Seki N (2013b) Epithelial–mesenchymal transition-related microRNA-200s regulate molecular targets and pathways in renal cell carcinoma. *J Hum Genet* **58**: 508–516.

Yoshino H, Seki N, Itesako T, Chiyomaru T, Nakagawa M, Enokida H (2013c) Aberrant expression of microRNAs in bladder cancer. *Nat Rev Urol* **10**: 396–404.

You H, Lin H, Zhang Z (2015) CKS2 in human cancers: clinical roles and current perspectives (Review). *Mol Clin Oncol* **3**: 459–463.

Zuiverloon TC, Nieuweboer AJ, Vekony H, Kirkels WJ, Bangma CH, Zwarthoff EC (2012) Markers predicting response to bacillus Calmette-Guerin immunotherapy in high-risk bladder cancer patients: a systematic review. *Eur Urol* **61**: 128–145.

Supplementary Information accompanies this paper on British Journal of Cancer website (http://www.nature.com/bjc)